Role of Calmodulin and Spc110p Interaction in the Proper Assembly of Spindle Pole Body Components

Holly A. Sundberg,* Loretta Goetsch,‡ Breck Byers,‡ and Trisha N. Davis*

*Department of Biochemistry and ‡Department of Genetics, University of Washington, Seattle, Washington 98195-7350

Abstract. Previously we demonstrated that calmodulin binds to the carboxy terminus of Spc110p, an essential component of the *Saccharomyces cerevisiae* spindle pole body (SPB), and that this interaction is required for chromosome segregation. Immunoelectron microscopy presented here shows that calmodulin and thus the carboxy terminus of Spc110p localize to the central plaque. We created temperature-sensitive *SPC110* mutations by combining PCR mutagenesis with a plasmid shuffle strategy. The temperature-sensitive allele *spc110-220* differs from wild type at two sites. The cysteine 911 to arginine mutation resides in the calmodulin-binding site and alone confers a temperature-sensitive phenotype. Calmodulin overproduction suppresses the temperature sensitivity of *spc110-220*. Furthermore, calmodulin levels at the SPB decrease in the mutant cells at the restrictive temperature. Thus, calmodulin binding to Spc110-220p is defective at the nonpermissive temperature. Synchronized mutant cells incubated at the nonpermissive temperature arrest as large budded cells with a G2 content of DNA and suffer considerable lethality. Immunofluorescent staining demonstrates failure of nuclear DNA segregation and breakage of many spindles. Electron microscopy reveals an aberrant nuclear structure, the intranuclear microtubule organizer (IMO), that differs from an SPB but serves as a center of microtubule organization. The IMO appears during nascent SPB formation and disappears after SPB separation. The IMO contains both the 90-kD and the mutant 110-kD SPB components. Our results suggest that disruption of the calmodulin-Spc110p interaction leads to the aberrant assembly of SPB components into the IMO, which in turn perturbs spindle formation.

Tʜᴇ microtubule-organizing center of *Saccharomyces cerevisiae* is the spindle pole body (SPB).[1] As seen by electron microscopy the SPB appears as a three-layered structure embedded within the nuclear envelope. The central plaque is flanked on either surface by the inner and outer plaques. Cytoplasmic microtubules emanate from the outer plaque, while nuclear microtubules emanate from the inner plaque. Besides functioning as the site of microtubule initiation for spindle assembly, the SPB plays additional roles in self-replication, mating, and spore wall formation (for review see Byers, 1981).

Cytologically, SPB duplication begins just before bud emergence when the satellite, a densely staining region of material, appears on the cytoplasmic surface of the half bridge, which abuts one edge of the single SPB. Coincident with bud emergence, the satellite-bearing single SPB is transformed into a pair of SPBs connected by a complete bridge (Byers and Goetsch, 1975). Both Cdc31p and Kar1p are components of the half bridge (Spang et al.,

1993, 1995), and both play essential roles in SPB duplication. Temperature-sensitive *cdc31* and *kar1* mutants arrest as large budded cells with a single enlarged SPB (Byers, 1981; Rose and Fink, 1987). Furthermore, Kar1p binds to Cdc31p and is required for Cdc31p localization to the SPB (Biggins and Rose, 1994; Spang et al., 1995).

Comparative analysis of *cdc31*, *mps1*, and *mps2* mutants has suggested a dependent pathway of functions that are required for SPB duplication (Winey et al., 1991). Briefly, *CDC31* functions are fully executed before α-factor arrest, whereas *mps1-1*, which similarly can arrest the duplication pathway before satellite formation, still causes a defect after release from α-factor arrest. *MPS1* is also required for normal half-bridge formation (Winey et al., 1991) and has recently been shown to encode a dual specificity protein kinase (Lauzé et al., 1995). *mps2* mutants also yield only one functional SPB, since a second SPB formed on the cytoplasmic surface of the half bridge does not undergo appropriate insertion into the nuclear envelope (Winey et al., 1991). Similarly, *ndc1* mutants assemble an SPB that fails to insert into the nuclear envelope. *NDC1* encodes a predicted integral membrane protein that localizes to the nuclear envelope, where it may aid insertion of the nascent SPB (Winey et al., 1993).

The separation of the duplicated SPBs to form the mi-

---

1. *Abbreviations used in this paper.* IMO, intranuclear microtubule organizer; MLCK, myosin light chain kinase; SPB, spindle pole body.

111

totic spindle requires the activities of the functionally redundant kinesin-related motor proteins Kip1p and Cin8p. Both motor proteins localize to the nuclear microtubules where they generate an outwardly directed force that separates the poles (Hoyt et al., 1992; Roof et al., 1992). Additionally, a cold-sensitive tubulin mutant (tub2-401) that is able to polymerize spindle microtubules but not astral microtubules remains proficient in SPB separation, supporting the idea that SPB separation occurs by sliding forces exerted on the spindle microtubules and does not require any activity of the astral microtubules (Sullivan and Huffaker, 1992).

An understanding of the assembly and the functions of the SPB and the mitotic spindle is still in its infancy. Recently, we demonstrated that calmodulin, a small Ca^{2+}-binding protein essential for cell proliferation, binds to a 28–amino acid segment in the carboxy terminus of Nuf1p/Spc110p (Geiser et al., 1993), an essential 110-kD component of the SPB (Kilmartin et al., 1993; Mirzayan et al., 1992). The interaction between calmodulin and Spc110p is required for proper spindle function (Geiser et al., 1993). Stirling and coworkers (1994) identified 13 residues (within these 28 residues) that match the consensus for a calmodulin-binding site and demonstrated that mutations within these 13 residues abolish calmodulin binding. We have used immunoelectron microscopy to show that calmodulin is localized to the central plaque of the SPB and therefore, the carboxy terminus of Spc110p is at the central plaque. To characterize further the functions of SPC110, we created temperature-sensitive Spc110p mutants. The present finding that one of these temperature-sensitive alleles, spc110-220, has a mutation in the calmodulin-binding site implicates calmodulin binding to Spc110p in appropriate assembly of SPB components. At the nonpermissive temperature, the spc110-220 mutant cells display aberrant aggregates of material that form in the nucleoplasm and interfere with spindle formation.

Materials and Methods

Media

SD complete medium, SD-uracil medium (Davis, 1992), and YPA medium (Davidow et al., 1980) were described previously. SD-uracil low adenine medium has 5 μg/ml adenine but is otherwise identical to SD-uracil medium.

Plasmids

Plasmids used in this study are listed in Table I. Plasmid pHS29 was created by digesting pMM31 (Geiser et al., 1993) with BamHI, filling the ends in with Klenow, and digesting with NarI. The BamHI–NarI fragment encoding SPC110 was ligated into the Asp718-ClaI sites of pHS28. Plasmid pHS28 is a derivative of pMM66 (gift of M. Moser) from which the SacI–HindIII fragment of the polylinker has been deleted. Plasmid pMM66 is identical to pRS316 (Sikorski and Hieter, 1989) except that the NcoI site has been removed from the URA3 gene.

To create a plasmid with a unique BamHI site in the SPC110 coding region, plasmid pHS29 was linearized by partial digestion with BclI and the ends filled in with Klenow. Then a BamHI 8-mer linker was ligated to the blunt ends. Digestion with BamHI removed the excess linker and the plasmid ends were ligated together. Restriction enzyme analysis identified a plasmid (named pHS32) with a unique BamHI site replacing the BclI site at the 3' end of SPC110.

Plasmid pHS39 is the isolate of spc110-220 identified in the screen for temperature-sensitive mutations in SPC110. Note that the BamHI site in the coding region of SPC110 of the parent plasmid pHS32 is no longer present in pHS39.

The spc110-220 integrating vector, pHS40, was created by replacing the 4.6-kb AlwNI fragment of pHS39 with the 2.6-kb AlwNI fragment of pRS306 (Sikorski and Hieter, 1989).

Plasmid pHS41 was created by replacing the 4.6-kb AlwNI fragment of pHS39 with the 4.8-kb fragment of pGF29 (gift of G. Zhu).

Site-directed mutagenesis (Kunkel et al., 1987) was used to introduce the C911R mutation into SPC110 in plasmid pHS29 to create pHS38.

Plasmid pTD52 was created by partially digesting pEL1 (Davis and Thorner, 1989) with EcoRI. The plasmid ends were filled in with Klenow and then ligated together. Restriction enzyme analysis identified a plasmid (pTD52) lacking the EcoRI site in the GAL promoter.

Strains

Strains used in this study are listed in Table II. Strain HSY10 was derived from CRY1 by integrating the spc110-220 gene at the SPC110 locus by a two-step gene replacement (Boeke et al., 1987) using plasmid pHS40 linearized with MluI. Integration was checked by Southern blot analysis. Presence of mutations S853G and C911R was confirmed by PCR amplification and sequencing.

Mutagenesis

Mutagenic PCR conditions were as described previously (Cadwell and Joyce, 1992). pHS29 linearized with PstI in URA3 served as the SPC110 template DNA. The mutagenic reaction mixture (50 μl) contained 10 ng linearized template DNA, 30 pmol of each PCR primer, reaction buffer

Table I. Plasmids Used in This Study

Plasmid	Parent plasmid	Relevant markers*	Source or reference
pGF29	pRS306	2 μm orgin (YEp24 EcoRI fragment) inserted at AatII site	gift of G. Zhu
pHS26	pTD29	SPC110 LYS2 ADE3, 2 μm orgin	(Geiser et al., 1993)
pHS29	pRS316	SPC110	This study
pHS32	pHS29	SPC110 with unique BamHI site towards 3' end	This study
pHS38	pHS29	spc110 with C911R	This study
pHS39	pHS32	spc110-220 (does not have unique BamHI site found in the parent plasmid)	This study
pHS40	pRS306	spc110-220	This study
pHS41	pGF29	spc110-220	This study
pJG115	pGF29	SPC110	gift of J. Geiser
pMR2486		GAL1-CDC31 URA3, 2 μm origin	gift of S. Biggins and M. Rose
pRS306		URA3, f1 origin	(Sikorski and Hieter, 1989)
pRS316		CEN6 ARSH4 URA3, f1 origin	(Sikorski and Hieter, 1989)
pTD17	YEp24	CMD1 URA3, 2 μm origin	(Zhu et al., 1993)
pTD52	pEL1	GAL1-CMD1 URA3 CEN4 ARS1	This study
pTD59	pUN50	CMD1 URA3 CEN4 ARS1	(Geiser et al., 1991)

*Unless stated otherwise, all markers from the parent plasmid are present in the new construct.

Table II. Strains Used in This Study

Strain	Genotype	Source or reference
CRY1	*MATa ade2-1oc can1-100 his3-11,15 leu2-3,112 trp1-1 ura3-1*	R. Fuller
JGY46	*MATa/MATα ade2-1oc/ade2-1oc can1-100/can1-100 his3-11,15/his3-11,15 leu2-3, 112/leu2-3,112 trp1-1/trp1-1 ura3-1/ura3-1*	(Geiser et al., 1991)
HSY2-1C (pHS26)	*MATα ade2-1oc ade3Δ can1-100 his3-11,15 leu2-3,112 lys2Δ::HIS3 spc110Δ:: TRP1 trp1-1 ura3-1*, carrying plasmid pHS26	(Geiser et al., 1993)
HSY10	*MATa ade2-1oc can1-100 his 3-11,15 leu2-3,112 spc110-220 trp1-1 ura3-1*	This study
TDY70-30A	*MATα ade2-1oc ade3Δ can1-100 leu2-3,112 trp1-1 ura3-1*	(Davis, 1992)
HSY11	HSY10 × TDY70-30A	This study
HSY11-3B	*MATα ade2-1oc can1-100 his3-11,15 leu2-3,112 spc110-220 trp1-1 ura3-1*	This study
HSY11-4D	*MATa ade2-1oc ade3Δ can1-100 leu2-3,112 spc110-220 trp1-1 ura3-1*	This study
HSY20	HSY11-3B × HSY11-4D	This study

(50 mM KCl, 10 mM Tris-HCl, pH 8.3, 0.01% gelatin), 7 mM MgCl$_2$, 0.5 mM MnCl$_2$, 0.2 mM each dATP and dGTP, and 1.0 mM each dCTP and dTTP. The reactions were preheated to 94°C for 1 min during which time 5 U *Taq* polymerase (Boehringer Mannheim Corp., Indianapolis, IN) were added. The reactions were cycled in an Ericomp TwinBlock™ System EasyCycler™ Series (San Diego, CA) for 30 cycles of 94°C for 1 min, 52°C for 1 min, and 72°C for 1 min.

Isolation of Temperature-sensitive Mutations in SPC110

Temperature-sensitive mutations in *SPC110* were created by combining a PCR mutagenesis technique (Muhlrad et al., 1992) with a plasmid shuffle strategy (Davis, 1990; Geiser et al., 1991). The procedure involved first amplifying the region of interest of *SPC110* (bp 2512–3306) under mutagenic PCR conditions. Then, plasmid pHS32 was digested with BamHI and BsrGI to create a 394-bp gap in the carboxy terminus of *SPC110*. The gapped pHS32 plasmid contains homology to both ends of the mutagenized PCR product. 1 µg of the mutagenized PCR product was cotransformed with 100 ng of gel-purified gapped BamHI–BsrGI pHS32 plasmid and 20 µl sheared salmon sperm DNA (20 mg/ml) into the plasmid shuffle indicator strain HSY2-1C (pHS26) (Geiser et al., 1993). Homologous recombination between the gapped pHS32 plasmid ends and the mutagenized DNA ends repairs the gapped plasmid, introducing mutations into *SPC110*. The transformants were plated at 37°C selecting for the repaired plasmid on SD-uracil low adenine medium. The indicator strain HSY2-1C (pHS26) was constructed such that colonies carrying a version of plasmid pHS32 in which the *SPC110* gene contained a temperature-sensitive mutation would remain solid red at 37°C and sector white at 21°C.

Isolation of a Synchronous Population of G1 Daughters

Yeast cultures (300 ml) were grown to 120–140 Klett units (4 × 10^7 cells/ml) in SD complete medium, which enhanced the percentage of unbudded cells as analyzed by phase-contrast microscopy. To separate the cells, the culture was sonicated for 30 s using a Braun-Sonic U sonicator (B. Braun Biotech, Inc., Allentown, PA) fitted with the standard probe generating a power output of 30 W. The cells were then fractionated by centrifugal elutriation. The sonicated culture was loaded at a flow rate of 50 ml/min using a Masterflex pump (Cole-Parmer Instrument Company, Niles, IL) into a JE-5.0 elutriator rotor spinning at 3,400 rpm in a model J-6B centrifuge (Beckman Instruments Inc., Palo Alto, CA) adapted for elutriation at 21°C. After loading, the cells were washed with 200 ml of water at a flow rate of 19 ml/min. Next, the rotor speed was lowered to 2,500 rpm, the flow rate increased to at least 50 ml/min, and the first 1 l fraction collected. The flow rate selected for collection of the first 1 l was determined by the cell size of the starting culture as measured by a Multisizer II (Coulter, Hialeah, FL). That is, the smaller the cells, the slower the flow rate at which the first fraction was eluted. Subsequent 1 l fractions were obtained by incremental increases of 4 ml/min in the flow rate. 0.1-ml samples of the successive fractions were analyzed for cell number and size distribution using a Coulter Multisizer II and examined for morphology by phase-contrast microscopy. The fraction chosen for the shift experiments typically contained 1–2 × 10^8 cells that were 95–100% unbudded. Calcofluor staining (Pringle et al., 1989) revealed that the cells ($n = 100$) did not have bud

scars and thus were daughters. The daughters were collected by filtration and resuspended in SD complete medium at a concentration of 10^7 cells/ml.

The synchrony obtained by elutriation is excellent. A wild-type population of early G1 daughters progressed through two cell cycles with tight synchrony as shown by measuring the DNA content (Fig. 1). Elutriation was chosen over α-factor arrest to obtain synchronous populations for two reasons. First, α-factor causes an arrest that occurs after the satellite appears on the SPB. An earlier cell population can be obtained by elutriation and thus satellite formation can be followed. Second, the properties of an SPB within a cell that is competent to mate after induction by α-factor may be different than the properties of an SPB in a cell that is progressing through the cell cycle. A complication of elutriation is that the daughters collected in successive experiments may not be exactly at the same stage of the cell cycle. The landmark we have used to align data from different elutriation shift experiments is the midpoint of S phase. For ease of comparison, we have set this as time = 0 min in subsequent figures. The midpoint of S phase is defined as the time when 50% of the cell population has replicated half its genome. The midpoint was extrapolated from a plot of time after elutriation vs the fraction of cells that had a DNA content greater than the midpoint between the G1 and G2 peaks of DNA content as measured by flow cytometry. This time point was easily and reproducibly identified.
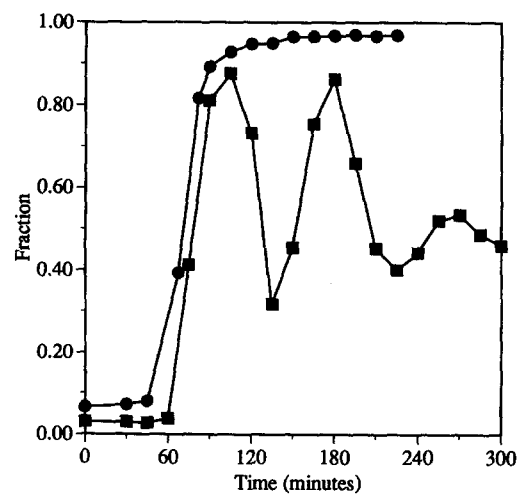

Figure 1. Timing of DNA replication for synchronous cultures of *spc110-220* mutant (HSY20) cells (●) and wild-type (JGY46) cells (■) synchronized in early G1 by elutriation as described in Materials and Methods. Time zero is the time of the shift to 37°C. At regular intervals, aliquots (100 µl) were mixed with 100% ethanol (200 µl) and prepared for flow cytometry as described in Materials and Methods. Both curves represent the fraction of the cell population that has replicated at least half of its genome.

Cytological Techniques

Yeast cells were prepared for flow cytometry and analyzed for DNA content as described (Muller, 1991). Cells were prepared for tubulin immunofluorescence as described (Davis, 1992) except that the primary antibodies were rat anti–α-tubulin ascites YOL1/34 diluted 1:200, and the secondary antibodies were goat anti–rat IgG conjugated to FITC (Boehringer Mannheim Corporation, Indianapolis, IN) diluted 1:100. Cells were prepared for SPB component immunolocalizations using a technique derived from a previous protocol (Rout and Kilmartin, 1990). The changes made in the methanol-acetone fixation protocol are described below. Spheroplasts were prepared from log phase cells by digestion with 0.25–0.75 mg/ml zymolyase 100T (ICN) in 1.1 M sorbitol/Wickerham's (2% glucose, 0.5% yeast extract, 0.5% malt extract, and 1% bactopeptone) at 37°C for 7.5 min or at 21°C for 30 min. Spheroplasts were pelleted at low speed in a microfuge and resuspended in 1.2 M sorbitol/100 mM sodium phosphate buffer pH 6.5 (SP). The spheroplasts were then mounted on polylysine-coated slides, washed three times in SP, and then fixed in methanol (−20°C) for 6 min before a 30-s immersion in acetone (21°C). DNA was stained with 4',6-diamidino-2-phenylindole (DAPI) at a concentration of 0.1 μg/ml. Stained cells were viewed with a Zeiss Axioplan fluorescent microscope (Carl Zeiss, Inc., Thornwood, NY).

Isolation of Yeast Nuclei

The yeast nuclear isolation procedure was derived from a previous protocol (Schultz, 1978). Yeast cultures (200 ml) were grown to 2×10^7 cells/ml in YPA medium at 21°C. To isolate nuclei from cells growing at the nonpermissive temperature, cultures (1.5–2.0×10^7 cells/ml) were shifted to 37°C for 1 h. The cells were harvested by centrifugation and incubated in 5 ml of a pretreat solution (Byers and Goetsch, 1991) for 10 min at room temperature. The cells were washed in 10 ml of 0.2 M phosphate-citrate buffer (0.17 M KH_2PO_4 and 30 mM sodium citrate to yield pH 5.8), followed by a wash in 10 ml of 10% glycerol, 0.05 M phosphate-citrate buffer, and 1.0 M sorbitol. The cells were spheroplasted with 100 μl glusulase (DuPont New England Nuclear®, Boston, MA) and 10 μl of 5 mg/ml zymolyase 100T (ICN Biomedicals, Costa Mesa, CA) in 1 ml of the previous wash solution. The spheroplasts were washed in 20 ml of 1.0 M sorbitol, 10% glycerol, 0.02 M potassium phosphate buffer, pH 6.5, and 0.5 mM $MgCl_2$. The spheroplasts were then lysed at room temperature by vortexing 10 s at maximum speed in 5 ml of 18% Ficoll (400,000), 0.02 M potassium phosphate buffer, pH 6.5, and 0.5 mM $MgCl_2$, and then immediately placed on ice. After 5 min, 5 ml ice cold HM buffer (2 M sorbitol, 0.02 M potassium phosphate buffer, pH 6.5, 0.5 mM $MgCl_2$, 8.4% Ficoll [400,000], and 24% glycerol) containing 0.2% NP-40 was added and the solution was vortexed to mix. Then an additional 10 ml ice cold HM buffer was added. The samples were spun at 12,000 g for 30 min at 4°C. The resulting supernatant was then spun at 65,000 g for 30 min at 4°C. The pellet was highly enriched for nuclei as determined by both light and electron microscopy.

Electron Microscopy

Cells were prepared for thin-section electron microscopy as described (Byers and Goetsch, 1991) except that the fixative was 3% (wt/vol) glutaraldehyde in buffer containing 50 mM potassium phosphate, pH 6.5, and 0.5 mM $MgCl_2$. The protocol used for immunoelectron microscopy of the isolated nuclei was derived from earlier protocols (Byers and Goetsch, 1991; Wright and Rine, 1989). Briefly, the isolated nuclei were fixed for 5 min at room temperature in 2 ml of 1% glutaraldehyde (EM grade), 1% formaldehyde (methanol free), 0.04 M potassium phosphate buffer, pH 7, and 1.0 mM $MgCl_2$. The samples were then incubated on ice for 30 min. The fixative was removed by three washes in 0.04 M potassium phosphate buffer, pH 7. The nuclei were resuspended in 2 ml of 50 mM ammonium phosphate and left at room temperature for 15 min, followed by two washes with distilled water. The nuclei were then fixed at room temperature for 30 min in 2 ml of 3% glutaraldehyde (biological grade), 50 mM potassium phosphate buffer, pH 6.5, and 1 mM $MgCl_2$. Next, the nuclei were washed three times in 0.1 M sodium acetate, pH 6.1, fixed with osmium tetroxide and uranyl acetate, dehydrated with ethanol, and embedded in Spurr resin as described (Byers and Goetsch, 1991). After thin sectioning, immunolabeling was performed as described (Wright and Rine, 1989) using affinity-purified anti-calmodulin antibodies (Brockerhoff and Davis, 1992) diluted 1:10. The secondary antibody is goat-anti–rabbit IgG conjugated to 15-nm-gold particles (Ted Pella, Inc., Redding, CA). Serial thin sections were viewed using a Philips EM300 electron microscope.

Results

Calmodulin Localizes to the Central Plaque of the SPB

The localization of calmodulin within the SPB was determined by immunoelectron microscopy on thin sections of isolated yeast nuclei using affinity-purified anti-calmodulin antibodies. The densely staining outer and central plaques were clearly visible while the inner plaque, though not darkly stained, was defined as the region occupied by the proximal ends of the nuclear microtubules. Approximately 50% of the SPBs ($n = 198$) were labeled by anti-calmodulin antibodies as detected by colloidal gold. Of these labeled poles, the majority of the gold particles (55%) overlapped at least a portion of the densely staining central plaque (Fig. 2), while 37% of the particles lay immediately adjacent to the nuclear surface of the central plaque (Fig. 2) and 8% labeled the region adjacent to the cytoplasmic surface of the central plaque. Thus, calmodulin localizes to the central plaque with a bias towards the nuclear side. Background immunogold staining was very low. Each entire nucleus contained on average only 0.6 gold particles that were not over the SPBs, whereas each labeled SPB (roughly 1% of the nuclear area) stained on average with 1.7 gold particles. Previous work has shown that the coiled-coil rod of Spc110p extends between the central and inner plaques (Kilmartin et al., 1993; Rout and Kilmartin, 1990). On the assumption that all of the calmodulin detected here is bound to the previously defined binding site in the carboxy terminus of Spc110p (Geiser et al., 1993; Stirling et al., 1994), this end of Spc110p must be situated at the central plaque while the amino terminus of Spc110p is localized on the inner plaque, from which nuclear microtubules emanate.

Isolation of Temperature-sensitive Mutations in SPC110

To characterize the function of SPC110, we created temperature-sensitive mutations in SPC110 by combining PCR mutagenesis (Muhlrad et al., 1992) with a plasmid shuffle strategy (Davis, 1990; Geiser et al., 1991) as described in Materials and Methods. Of the 18,400 colonies screened at 37°C, 1602 solid red colonies were isolated and patched at 37°C and 21°C to check for sectoring. Sixteen colonies remained red at 37°C and sectored at 21°C. The repaired SPC110 plasmid was rescued from each colony, and 11 of the 16 plasmids conferred temperature sensitivity when retransformed into the plasmid shuffle indicator strain.

One allele contained two missense mutations: serine 853 to glycine (S853G) and cysteine 911 to arginine (C911R). A strain carrying both mutations (spc110-220) integrated at the SPC110 locus grows well at 34°C, but does not grow at 37°C. A yeast strain carrying only the C911R mutation also grows well at 34°C, but does not grow at 37°C. Thus, the C911R mutation alone confers the same temperature-sensitive phenotype as spc110-220. A diploid homozygous for spc110-220 grows poorly at 32°C and does not grow at 34°C and above. A diploid heterozygous for spc110-220 grows well at 37°C, demonstrating that spc110-220 is recessive.
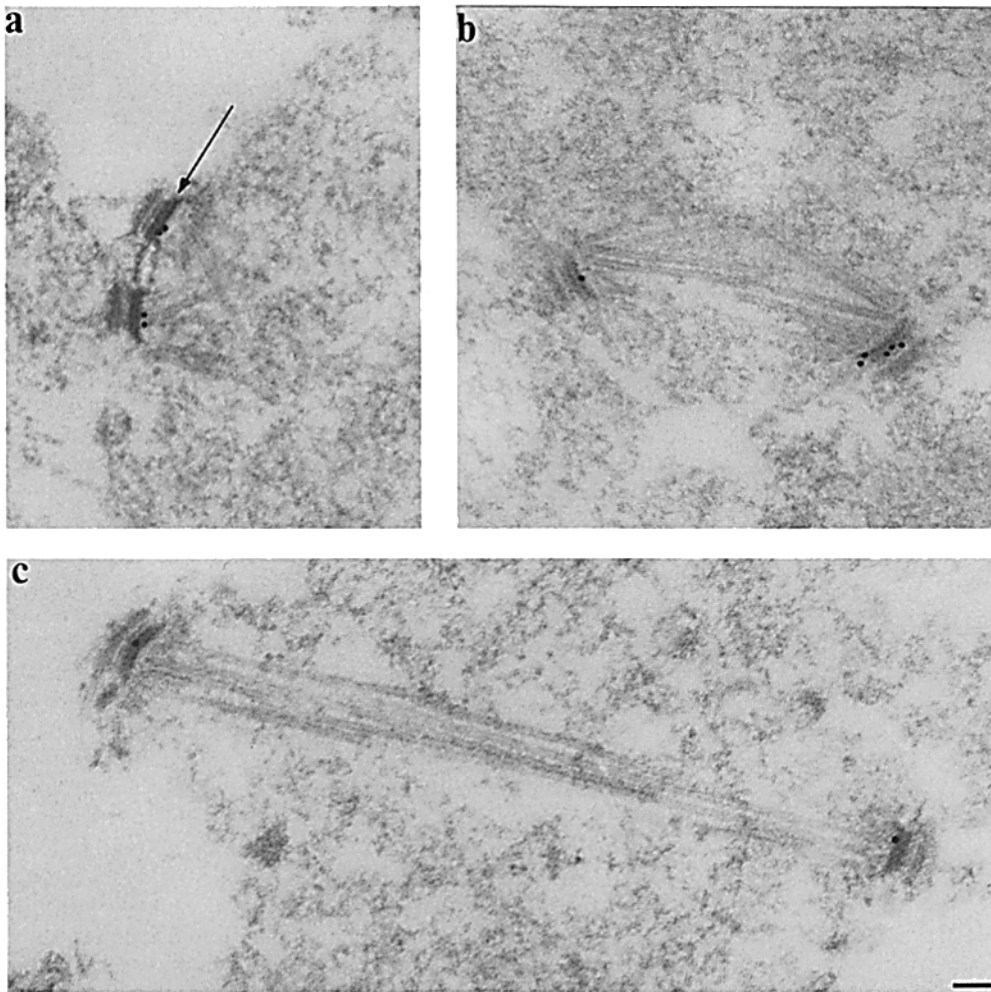
Figure 2. Calmodulin localizes to the central plaque of the SPB. Immunoelectron microscopy of isolated wild-type (JGY46) nuclei labeled with affinity-purified anti-calmodulin antibodies as described in Materials and Methods. (*a*) Duplicated, paired SPBs. The arrow indicates the location of the central plaque. (*b*) Short complete spindle. (*c*) Elongated spindle. Bar, 0.1 μm.

Overexpression of CMD1 Suppresses spc110-220

The C911R mutation resides in the calmodulin-binding region of Spc110p (Geiser et al., 1993; Stirling et al., 1994). We tested whether expression of plasmid-borne *CMD1* (the gene encoding calmodulin) could suppress the temperature sensitivity of the *spc110-220* homozygous diploid. Although a single-copy plasmid encoding *CMD1* did not relieve the temperature-sensitive phenotype, either a high-copy number plasmid encoding a 17-fold excess of calmodulin or a single-copy plasmid encoding the *CMD1* open reading frame under control of the *GAL1* promoter (80-fold excess when grown on 2% galactose) (Davis and Thorner, 1989) allowed growth at 37°C. Suppression is specific to calmodulin because a plasmid containing *CDC31*, which encodes a Ca^{2+}-binding protein involved in SPB duplication, expressed under control of a *GAL1* promoter (gift of S. Biggins and M. Rose) did not suppress the temperature sensitivity of the *spc110-220* homozygous diploid (data not shown). A simple hypothesis for the reason overexpression of calmodulin suppresses *spc110-220* is that the cysteine-to-arginine mutation in the calmodulin-binding site of Spc110-220p reduces the affinity of calmodulin binding. Thus, elevating the levels of calmodulin in the mutant strain helps overcome this decreased affinity.

Calmodulin Levels at the SPB Decrease at the Nonpermissive Temperature

We used immunoelectron microscopy of isolated yeast nuclei stained with affinity-purified anti-calmodulin antibodies to determine relative calmodulin levels at the SPB at permissive and nonpermissive temperatures (Table III). We found that exposure of the *spc110-220* mutant to the restrictive temperature caused a striking reduction in the number of immunolabeled SPBs. The number of gold particles per SPB in the *spc110-220* mutant was reduced 3.6-fold by incubation for 1 h at 37°C relative to a 1.1-fold reduction for wild-type SPBs.

Table III. Immunogold Labeling of Calmodulin at the SPB

	Total SPBs	Poles with particles	Total gold particles on SPBs	Gold particles per SPB
wild-type 21°C	104	53	97	0.93
wild-type 37°C	94	52	83	0.88
spc110-220 21°C*	95	47	82	0.86
spc110-220 37°C*	115	26	28	0.24

*Background is the same as wild type.
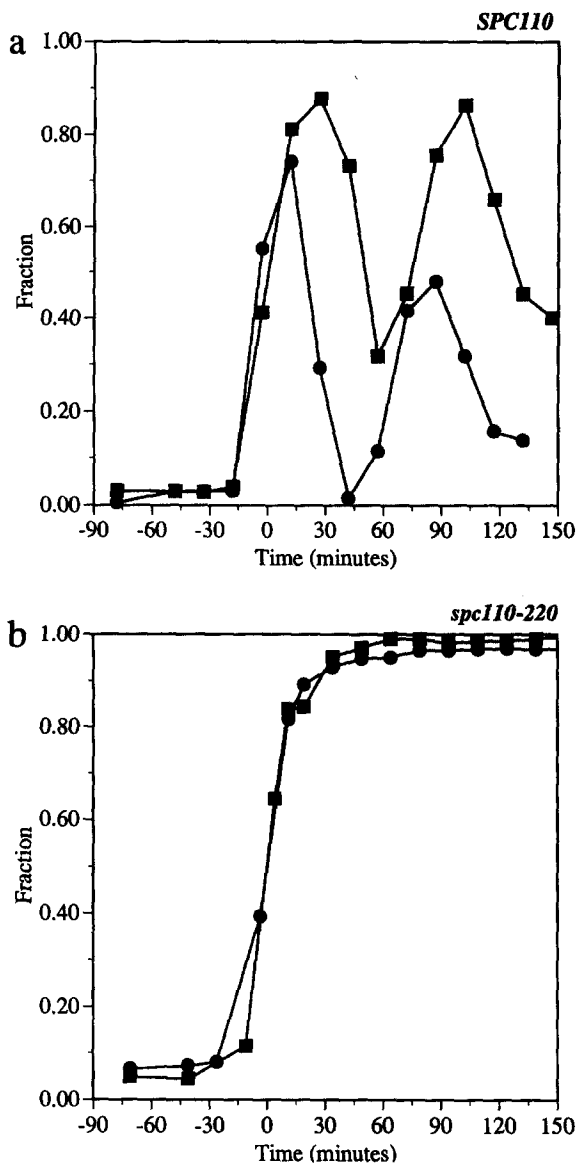
SPC110

spc110-220

Figure 3. Progression through the cell cycle of synchronous cultures of wild-type cells (a) and spc110-220 mutant cells (b). A population of cells in early G1 was obtained from cultures of strains JGY46 and HSY20 by centrifugal elutriation as described in Materials and Methods and then shifted to 37°C. At regular intervals, aliquots (100 μl) were mixed with 100% ethanol (200 μl) and prepared for flow cytometry as described in Materials and Methods. Additional aliquots (200 μl) were mixed with formaldehyde to a final concentration of 3.7%. The morphology of the cells was determined by phase-contrast microscopy. 200 cells were counted for each time point. The landmark used to align data from different elutriation shift experiments is the midpoint of S phase (see Materials and Methods). For ease of comparison, we have set this as time = 0 min in this and subsequent figures. (a) SPC110: the wild-type culture progresses through two cell cycles as shown by plotting either ■, the fraction of the cell population that has replicated at least half of its genome, or ●, the fraction of cells with small buds. (b) spc110-220: the spc110-220 mutant culture arrests in the first cell cycle with a G2 content of DNA and large buds as best shown by plotting either ■, the fraction of the cell population that has replicated at least half of its genome, or ●, the fraction of cells with buds of any size. Note in both wild-type and mutant cultures, bud emergence coincides with the midpoint of S phase (time = 0 min). In the mutant culture, the midpoint of S phase is 71 min after the shift to 37°C.

Cell Cycle–specific Defects of the Temperature-sensitive spc110-220 Mutant

When shifted to the nonpermissive temperature, cultures of haploid or homozygous diploid spc110-220 strains, whether asynchronous or synchronous, arrest as large budded cells with a G2 content of DNA. Further characterization of this arrest was performed with a homozygous diploid because of greater ease in visualizing SPBs in larger cells. All subsequent analyses were performed with synchronous populations of cells isolated by elutriation. At the nonpermissive temperature, spc110-220 homozygous diploid cells progressed through S phase and completed bud emergence and bud growth at rates similar to wild-type cells (Figs. 1 and 3, and data not shown). By 2 h after the shift to 37°C, the culture had accumulated 87% large-budded cells and a G2 content of DNA, and the cells remained in this state after 4 h of incubation at 37°C (97% large budded cells). DAPI staining of fixed cells revealed that the DNA remained near the bud neck or spanned it and had not segregated (Fig. 4). This phenotype suggested a classic arrest in G2/M, but immunofluorescent staining of the microtubules did not reveal the short spindle expected at a G2/M arrest. Instead, many broken spindles were seen and excessive numbers of microtubules were often present (Fig. 4). Furthermore, after 4 h, only 23% of the mutant cells remained viable, as determined by their ability to form colonies when returned to permissive temperature (data not shown).

We first tested if the spc110-220 mutant showed defects in phosphorylation of Spc110p. Studies of synchronous wild-type cultures have revealed that Spc110p is phosphorylated in a cell cycle–dependent manner (Friedman et al., 1996). Immunoblot analysis of a synchronous population of spc110-220 cells in early G1 released at 37°C revealed that the majority of Spc110-220p undergoes the cell cycle–dependent phosphorylation (Fig. 5).

At 21°C, Spc110-220p levels in an spc110-220 homozygous diploid are comparable to Spc110p levels in a wild-type diploid. The amount of Spc110-220p present in an asynchronous spc110-220 homozygous diploid strain growing at 37°C for 1 h is approximately twofold lower than the level of Spc110p present in a wild-type diploid growing under the same conditions (data not shown). We do not believe that the temperature sensitivity of spc110-220 is due to this slight decrease in protein levels because extra copies of spc110-220 expressed from either single-copy or high-copy number vector did not suppress the temperature sensitivity. As a control, wild-type SPC110 expressed from either a single-copy plasmid or a high-copy number plasmid allowed the homozygous spc110-220 diploid to grow at 37°C (data not shown).

Electron Microscopy Defines the Presence of an Aberrant Microtubule-organizing Center, the Intranuclear Microtubule Organizer

Spindle pole bodies and spindle morphology in a synchronous population of the spc110-220 homozygous diploid cells were examined in greater detail by electron microscopy. Examination of serial thin sections of the spc110-220 strain fixed after incubation at the nonpermissive temperature revealed the presence of an aberrant nuclear struc-

Tubulin   DNA
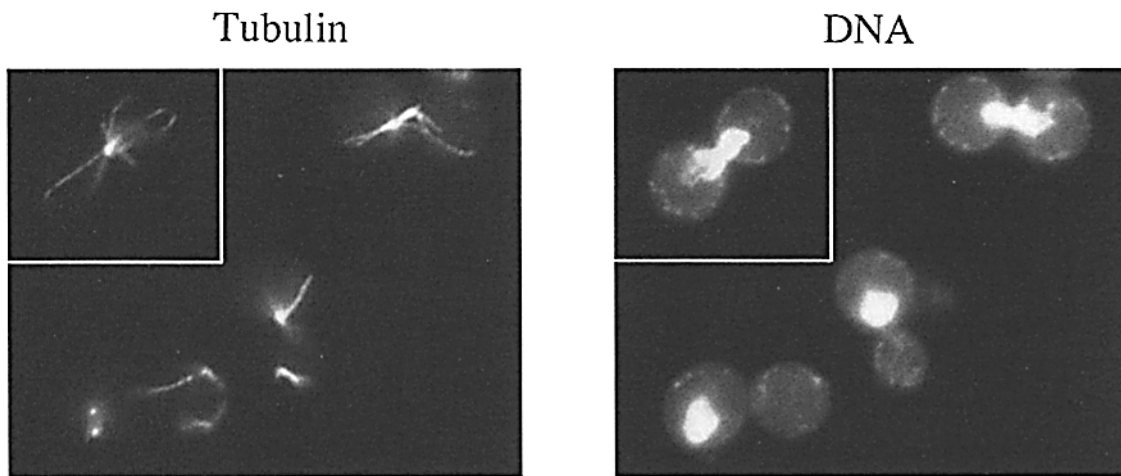
Figure 4. Tubulin immunofluorescence of *spc110-220* mutant cells. A population of cells in early G1 was obtained from a culture of strain HSY20 by centrifugal elutriation as described in Materials and Methods, and then shifted to 37°C. Samples taken 151 min after the midpoint of S phase were stained for immunofluorescence as described in Materials and Methods. Bar, 5 μm.

ture that differs from an SPB but similarly appears to serve as a center of microtubule organization (Fig. 6). This structure, which we term an Intranuclear Microtubule Organizer (IMO), not only lacks the well-defined structure of an SPB, but usually is larger and resides entirely within the nucleoplasm, rather than being embedded in the nuclear envelope. Whether the IMO can nucleate microtubule polymerization rather than capture microtubules is discussed later.

IMOs form as the new SPB forms (Fig. 7) and first appear in cells in which the single SPB has a satellite. By the stage (time = −25 min, relative to the midpoint of S phase [see Materials and Methods]) when ~50% of the single SPBs have a satellite, 36% (4/11) of the nuclei contained an IMO. IMO formation continues during SPB duplication. When the majority of the nuclei had duplicated SPBs in the side-by-side configuration (time = −5 min), 69%

(34/49) of the nuclei contained an IMO, which generally had its microtubules directed toward the duplicated SPBs (Fig. 6, *a* and *b*). At later stages, the IMO disappeared. A densely staining structure that was similar in appearance to the IMO but was not associated with any microtubules was detectable in roughly 14% of the mutant nuclei at 37°C at all time points except the starting population.

The IMO has never been observed in a wild-type strain growing at 21°C or 37°C, or in an *spc110-220* homozygous diploid strain growing at 21°C. A heterozygous *spc110-220* diploid also does not exhibit an IMO when incubated at 37°C. However, a dense structure devoid of microtubules was detectable in 8 out of 11 heterozygous *spc110-220* diploid cells with either duplicated SPBs or short complete spindles (data not shown).

Loss of Viability Correlates with the Disappearance of Normal Spindles

Loss of viability of synchronous *spc110-220* cells shifted to 37°C correlates with the disappearance of spindles that appeared normal when examined by electron microscopy (Fig. 7). The single SPBs at the start of the experiment appeared morphologically normal. Additionally, the duplicated poles formed at the nonpermissive temperature were indistinguishable from one another and appeared to be nucleating an appropriate number of microtubules, even in the presence of the IMO. At these early times (< −12 min) all of the cells were viable and formed colonies when returned to the permissive temperature. Even the initial appearance of the IMO did not kill the cells. When 69% of the cells contained an IMO (time = −5 min), 93% of the cells were still viable (Fig. 7). The greatest loss of viability occurred during SPB separation (Fig. 7). By the time SPB separation was complete (time = 40 min), only 56% of the cells were viable. At this time, the duplicated SPBs had separated to give rise to broken spindles in 50% of the cells (8/16) and short complete spindles in the other 50%. Both SPBs of a broken spindle remain within the nuclear envelope, but the SPBs are not properly oriented to face one another. Instead, microtubules ema-
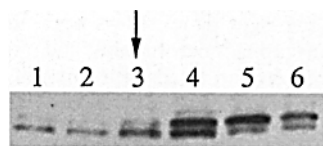
Figure 5. Immunoblot analysis of Spc110-220p in a synchronous culture. A population of early G1 cells of strain HSY20 was obtained by centrifugal elutriation as described in Materials and Methods, and then shifted to 37°C. Every 30–60 min 1 ml of the synchronous culture was collected and total cell protein extracts prepared as described (Wright et al., 1989). Immunoblot analysis was performed as described (Friedman et al., 1996). Time zero is the midpoint of S phase. For each lane, total cell protein extracts prepared from 1 ml of the synchronous culture were loaded. Lane *1* is the starting population of cells (time = −74 min) collected by elutriation. The lower and predominant band of lane *1* is Spc110-220p that has not undergone the cell cycle–dependent phosphorylation. (Lane *2*) time = −44 min. The ↓ marks the time when 50% of the nuclei examined had duplicated SPBs. (Lane *3*) time = −14 min. At time = 16 min, half of the Spc110-220p has been modified by the cell cycle–dependent phosphorylation, creating a protein of different mobility which migrates as the upper band of lane *4*. Phosphorylation of Spc110-220p occurs as the mitotic spindle forms. (Lane *5*) time = 46 min. At time = 106 min, nearly 70% of the cells have lost viability (lane *6*).
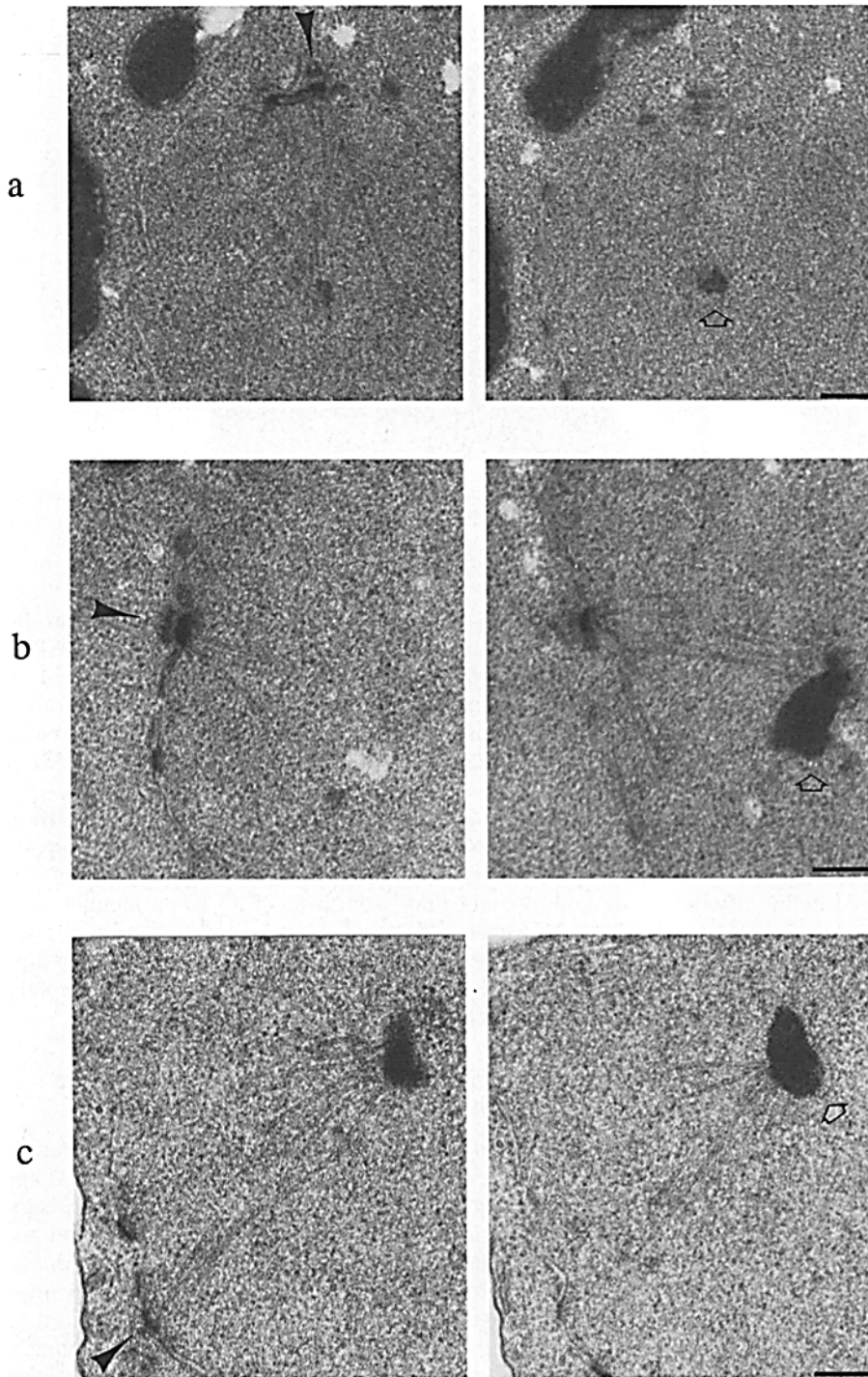
Figure 6. Electron micrographs of the *spc110-220* mutant at 37°C showing examples of the intranuclear microtubule organizer (IMO). Two thin sections of each of the three different cells (*a*, *b*, and *c*) are shown. Filled arrowheads indicate the location of SPBs and open arrows indicate the location of IMOs. (*a*) The thin section on the left shows duplicated paired SPBs whose microtubules are pointed towards a small dense structure that also appears to be nucleating microtubules at time = −5 min. The adjacent section that is shown in the right panel reveals the size of the IMO. (*b*) The thin section on the left shows an SPB nucleating microtubules (time = 5 min). Not shown is the thin section between the left and right panels which depicts the bridge structure joining the paired SPBs. The thin section in the right panel shows both an SPB nucleating microtubules and an IMO that is associated with microtubules. (*c*) The thin section on the left shows an SPB mispairing with an IMO at time = 40 min. The adjacent section shown in the right panel provides a striking view of the IMO nucleating microtubules. Bar, 0.2 μm.

nating from the IMO are often seen to interact with those emanating from one or both of the spindle pole bodies to form an aberrant spindle-like array (Figs. 6 *c* and 8). We propose that interactions between microtubule arrays emanating from either SPB can be displaced by interactions with the IMO-associated array, thus leading to formation of a broken spindle. The 50% of the cells that are viable when SPB separation is finished are presumably those that appear to have complete spindles with both poles embedded in the nuclear envelope as shown in Fig. 9. However, even these normal-appearing short complete spindles may have suffered some damage that causes them to break at later times because the fraction of cells with complete spindles decreases to 30% at 70 min. The correlation between the loss of viability and the appearance of broken spindles is striking throughout the time course (Fig. 7).

Immunofluorescence Also Reveals an Extra Center of Microtubule Organization

The IMO could also be detected in the *spc110-220* mutant cells at the nonpermissive temperature by immunofluores-
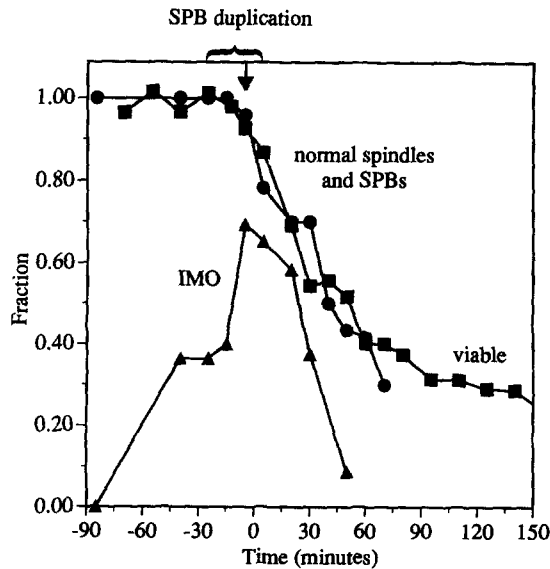
Figure 7. Accumulation of the IMO. Loss of viability of the spc110-220 mutant correlates with the disappearance of normal spindles and SPBs. The spc110-220 mutant culture (strain HSY20) was synchronized in early G1 by elutriation as described in Materials and Methods and released at 37°C. At regular intervals, aliquots were removed, sonicated, and titered for colony forming units at 21°C on YPD. Aliquots were also processed for thin-section electron microscopy as described in Materials and Methods. Time zero is the midpoint of S phase. The time when duplicated SPBs in the side-by-side configuration arise is bracketed. SPB separation begins at the time marked by the arrow (↓) and is completed by time = 40 min. Between 9 and 49 nuclei (average of 20) were examined for each time point. ▲, fraction of cells with an IMO; ■, fraction of cells viable when plated at the permissive temperature; ●, fraction of cells with normal spindles and SPBs (equal to 1 − [the fraction of cells with broken spindles]). At early time points, all cells had single SPBs or duplicated SPBs that appeared morphologically normal. At late time points, the cells had short complete spindles or broken spindles. All unbroken spindles were scored as normal even if the nucleus contained an IMO.

cence microscopy using two different fixation protocols. Anti-tubulin antibody staining of formaldehyde fixed unbudded mutant cells at 37°C revealed an aberrant structure. An unbudded wild-type cell has a single SPB nucleating microtubules; this appears by anti-tubulin staining as an array emanating from a single focus (Fig. 10 a). Although the starting population of elutriated spc110-220 mutant cells also exhibited a single center of microtubule organization, 7% of the unbudded spc110-220 cells contained two immunofluorescent centers of tubulin organization 40 min before half of the cells had gained duplicated SPBs as determined by electron microscopy (time = −56 min). These two centers of anti-tubulin staining appeared as separate entities with no visible interconnections between them (Fig. 10 b). 15 min later, the number of mutant unbudded cells with two foci had increased to 12%. We propose that one center of tubulin organization is the single SPB and the other is an IMO. Two unconnected centers of tubulin immunofluorescence were never found in the wild-type cells at any stage of the cell cycle.
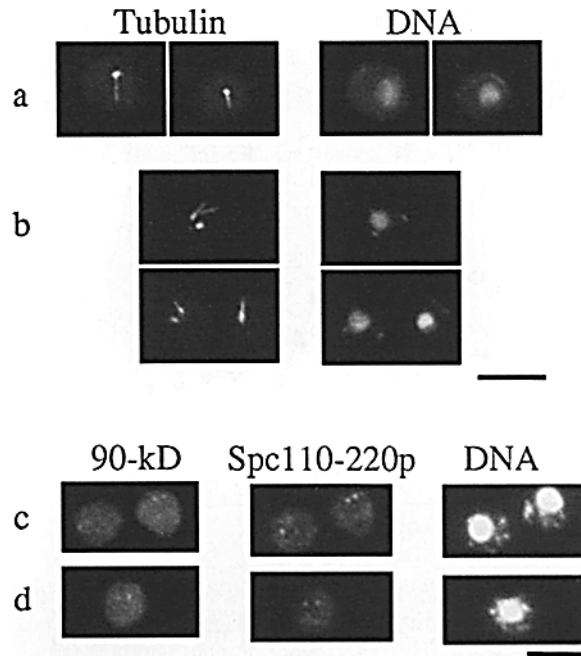
The IMO could also be detected by immunofluores-
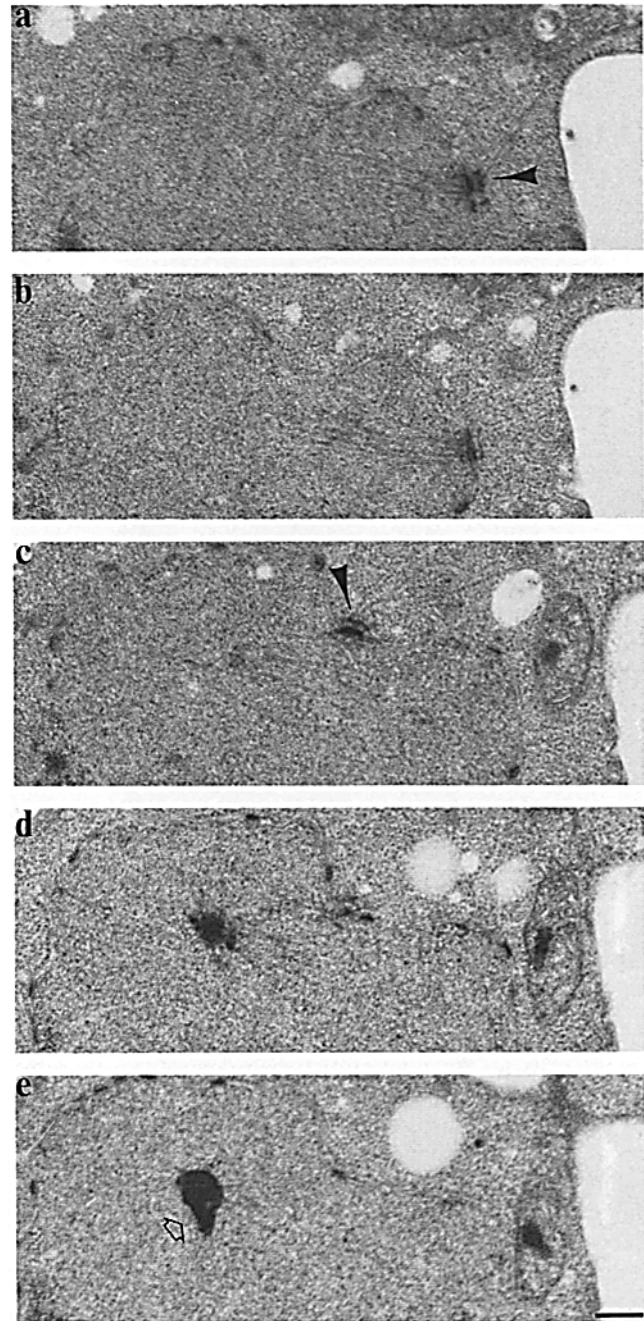
Figure 8. Electron micrographs of a serial thin section showing the IMO and a broken spindle in the nucleus of an spc110-220 mutant cell at 37°C (time = 5 min). Filled arrowheads indicate the location of SPBs and the open arrow indicates the location of the IMO. (a) An SPB nucleating microtubules is visible. The microtubules are directed towards the region where the IMO is located (d and e). (b) The array of nuclear microtubules is emanating from the SPB towards the region of the IMO. The thin section between b and c reveals numerous microtubules in the nucleoplasm (data not shown). (c) The second SPB is seen at the top edge of the nuclear envelope. Only a few microtubules are visible emanating from this second SPB. The IMO is also detectable in the center of the nucleus. (d) The IMO is associated with microtubules directed towards the SPB in a. (e) The final thin section reveals the size of the IMO. Bar, 0.2 μm.
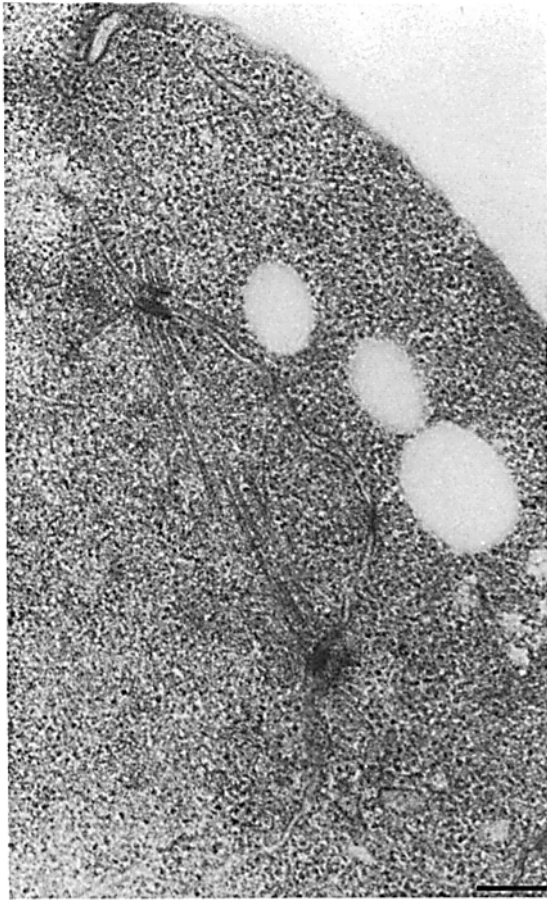
Figure 9. Electron micrograph showing a complete spindle in the *spc110-220* mutant at 37°C at time = 30 min. Bar, 0.2 μm.

Figure 10. Immunofluorescent staining with anti-tubulin antibodies, anti–90-kD antibodies, and anti-Spc110p antibodies reveals the IMO at 37°C in *spc110-220* mutant cells. DNA was stained with DAPI as described in Materials and Methods. (*a* and *b*) Tubulin immunofluorescence. Samples were stained for tubulin immunofluorescence as described in Materials and Methods. (*a*) Tubulin immunofluorescence of unbudded wild-type cells (time = −48 min) reveals a single focus of microtubule organization. (*b*) Tubulin immunofluorescence of unbudded *spc110-220* cells (time = −41 min) reveals two centers of microtubule organization in a fraction of the cells. One center of organization is the single SPB, and presumably, the other center is an IMO. (*c* and *d*) 90-kD staining and 110-kD staining of unbudded *spc110-220* mutant cells reveals two dots of colocalized staining in a fraction of the cells. One dot of staining represents the single SPB and the other dot represents the IMO. The cells were stained with affinity-purified anti-Spc110p antibodies and anti–90-kD antibodies. The primary antibodies were a mixture of mouse monoclonal anti-90 kD antibodies (diluted 1:10; gift of J. Kilmartin) and affinity-purified anti-Spc110p antibody (1:3,000) (Friedman et al., 1996). The secondary antibodies were a mixture of rhodamine-conjugated affinity-purified sheep IgG anti–mouse Ig (20 μg/ml; Boehringer Mannheim Corp., Indianapolis, IN) and fluorescein-conjugated goat anti–rabbit antibody ([1:1,000]; Boehringer Mannheim). (*c*) time = −94 min. (*d*) time = −79 min. Bar, 5 μm.

cence microscopy of methanol-acetone fixed *spc110-220* mutant cells at the nonpermissive temperature, thereby enabling us to identify some of its molecular constituents. For clarity, we first describe the events of spindle formation as seen by immunofluorescent staining with antibodies directed against the 90-kD SPB component (gift of J. Kilmartin) in our synchronized wild-type cells. The 90-kD SPB component is localized to the outer and inner plaques of the SPB (Rout and Kilmartin, 1990). An unbudded wild-type cell has a single SPB nucleating microtubules and thus we see only a single dot of 90-kD staining by fluorescence microscopy. Duplicated, paired side-by-side SPBs similarly appear as a single (but larger) dot by anti-90 kD staining. When the bud diameter is about one-third that of the mother cell, the 90-kD staining resolves the two SPBs as two dots of staining, thus marking the poles of the short spindle. Wild-type spindle formation occurs 9 min after the midpoint of S phase as determined by the appearance of two SPBs staining with the anti–90-kD component antibodies (Fig. 11).

The starting population of *spc110-220* mutant cells contained one dot of anti-90 kD staining corresponding to the single pole as expected. However, two dots of 90 kD staining were detected in unbudded cells shortly after the shift to 37°C (Fig. 10, *c* and *d*). The number of mutant cells with two dots of 90-kD staining had increased to 35% before any of the mutant cells had duplicated their SPBs as deter-

mined by electron microscopy (time = −35 min) (Fig. 12). Staining the *spc110-220* mutant cells with anti-Spc110p antibodies also revealed extra dots of staining arising at this early stage of the cell cycle (Figs. 10, *c* and *d* and 12). We also stained the *spc110-220* mutant cells with anti-calmodulin antibodies and did not detect calmodulin in either the IMO or the SPBs.
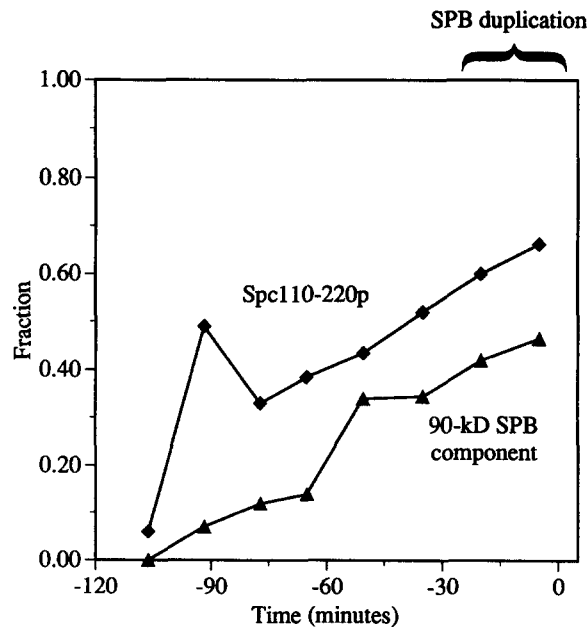
We believe that the extra dot of staining detected by the anti–90-kD antibodies in the unbudded *spc110-220* mutant cells is the IMO. The number of extra dots of 90 kD staining at early times after the shift to 37°C correlates well with the number of IMOs detected by electron microscopy (compare Fig. 7 IMOs with Fig. 12 90-kD staining). Interestingly, there is a greater fraction of cells showing two
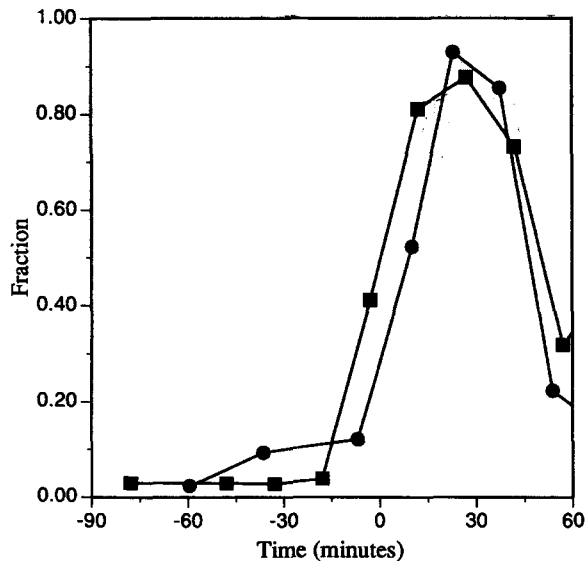
Figure 11. Timing of wild-type spindle formation. A population of cells in early G1 was obtained from strain JGY46 by centrifugal elutriation as described in Materials and Methods and was shifted to 37°C. At regular intervals, samples were removed and prepared for immunofluorescence as described in Materials and Methods. Samples were stained with anti-90 kD antibodies as described in Fig. 10. Time zero is the midpoint of S phase and is the landmark chosen to align the data from different elutriation experiments. The timing of spindle formation as assayed by two dots of anti-90 kD staining in wild-type cells. ■, fraction of the wild-type cell population that has replicated at least half of its genome; ●, fraction of wild-type cells with two dots of anti-90 kD staining.

Figure 12. Timing of incorporation of Spc110-220p and the 90-kD SPB component into the IMO. A population of cells in early G1 was obtained from strain HSY20 by centrifugal elutriation as described in Materials and Methods and shifted to 37°C. At regular intervals, samples were removed and prepared for immunofluorescence as described in Materials and Methods. Samples were stained with affinity-purified anti-Spc110p antibodies and anti-90-kD antibodies as described in Fig. 10. Note that this *spc110-220* starting population was earlier in G1 than those shown previously. Time zero is the midpoint of S phase. The timing of spindle pole body duplication as determined by electron microscopy is bracketed. Immunofluorescent staining with antibodies directed against the 90-kD SPB component and Spc110-220p reveals extra dots of staining in *spc110-220* mutant cells. In a cell that contains two dots of staining before the time of SPB duplication, one dot is the SPB and the other is the IMO. ▲, fraction of *spc110-220* mutant cells with two dots of 90-kD component staining; ◆, fraction of *spc110-220* mutant cells with two dots of Spc110-220p staining.

dots of staining with the anti-Spc110p antibodies than anti–90-kD antibodies (Fig. 12). Thus, some of the structures that contain the 110-kD component must not contain the 90-kD component, suggesting the mutant Spc110-220p first assembles into an aberrant structure that only later attracts the 90-kD component. The number of unbudded mutant cells observed with two tubulin foci is lower than the number of cells with two structures containing the 90-kD component. However, the boundaries of the larger anti-tubulin staining structures are less defined than the anti–90-kD stained dots making it more difficult to distinguish two distinct centers of tubulin organization. Thus, the number of cells with two foci determined by tubulin immunofluorescence is a minimal estimate. We attempted immunolabeling thin sections of yeast and of isolated nuclei using anti–90-kD antibodies and anti-Spc110p antibodies to confirm the presence of these spindle pole components in the IMO by electron microscopy, but the level of staining was inadequate for analysis.

In performing colocalization studies using anti–90-kD antibodies and anti-Spc110p antibodies, we found that 34% of the structures that stain with the anti–90-kD antibodies 34 min (time = −50 min) before half of the cells had duplicated SPBs did not stain with the anti-Spc110p antibodies. This absence of a one-to-one correspondence in colocalization experiments at early time points may be artifactual since the staining of the 110-kD component is not as robust as that of the 90-kD component, especially in

cells in G1. Even in wild-type cells in G1, as many as 20% of the spindle poles that stain with the anti–90-kD antibodies do not stain detectably with anti-Spc110p antibodies. At times after SPB duplication, however, Spc110-220p staining colocalized with 90-kD staining in every case examined (*n* = 106). Three structures stained with both anti–90-kD antibodies and anti-Spc110p antibodies in 11% of the cells 30 min (time = 25 min) after pole separation began and in 6% of the cells 45 min after pole separation began. Presumably, two dots of immunofluorescent staining represent the now separated SPBs and the third dot represents the IMO. The fact that both SPBs stain with anti-Spc110p antibodies demonstrates that some Spc110-220p is incorporated into the nascent SPB.

Discussion

Immunoelectron microscopy has previously defined key features of macromolecular organization in the yeast spindle pole body (SPB). Rout and Kilmartin (1990) prepared monoclonal antibodies against cellular fractions enriched

in SPBs. Immunoelectron microscopy using these antibodies revealed the localization of the SPB components (Rout and Kilmartin, 1990). The 42-kD SPB component is localized to the central plaque which lies in the plane of the nuclear envelope (Rout and Kilmartin, 1991). The 90-kD component is localized to both the outer and inner plaques (Rout and Kilmartin, 1990) from which microtubules emanate. The 80-kD component is localized to spindle microtubules close to the SPB. The coiled-coil rod of the 110-kD component has been shown to act as a spacer between the central plaque and the inner plaque (Kilmartin et al., 1993), but the orientation was not established. We have previously shown that calmodulin binds to the carboxy terminus of the 110-kD SPB component, Nuf1p/Spc110p (Geiser et al., 1993; Stirling et al., 1994). Here we demonstrate that calmodulin localizes to the central plaque, thus indicating that the carboxy terminus of Spc110p is located at the central plaque. Furthermore, we show that perturbation of the interaction between Spc110p and calmodulin results in misassembly of SPB components.

One of our temperature-sensitive *SPC110* alleles, *spc110-220*, contains a cysteine-to-arginine change in the calmodulin-binding site that confers temperature sensitivity. The calmodulin-binding site in Spc110p is a basic amphipathic α-helix similar to calmodulin-binding sites found in other calmodulin-binding proteins. In these other proteins, both the hydrophobic residues and the positively charged residues participate in binding calmodulin (Ikura et al., 1992; Meador et al., 1992; Meador et al., 1993). The cysteine-to-arginine mutation in *spc110-220* disrupts the hydrophobic face of the amphipathic α-helix of Spc110p and thus is predicted to decrease the affinity of Spc110-220p for calmodulin. Given the nature of this mutation and the fact that overproduction of calmodulin suppresses the temperature sensitivity of *spc110-220*, we conclude that binding of calmodulin to Spc110-220p at the nonpermissive temperature is defective. In support of this conclusion, we find a reduced level of calmodulin at the SPB in the mutant at the restrictive temperature.

The cellular consequences of this defect were examined by cytological analysis. When a synchronous population of *spc110-220* mutant cells was shifted to 37°C, the cells arrested with large buds and a G2 content of DNA, consistent with a block in mitosis. Electron and immunofluorescence microscopy of the mutant cells have revealed the presence of an intranuclear microtubule organizer, or IMO. The IMO appears at the time that the second SPB is forming and then disappears after the SPBs separate. The IMO is structurally distinct from an SPB, but it shares with the SPB the property that microtubules emanate from it. As judged from immunofluorescence, the IMO contains both the 90-kD component and the mutant 110-kD component. Proof that the IMO is nucleating microtubules and not capturing them would require an in vitro assay for microtubule nucleation on purified IMOs and is beyond the scope of this paper. However, three attributes of the IMO suggest that it nucleates microtubules. First, the IMO often is located some distance from the SPBs and appears to have microtubules radiating outwards. Second, the IMO contains the 90-kD SPB component that is normally found at the central and inner plaques, two sites at which microtubules are nucleated. Finally, when unbudded mutant cells first begin to exhibit two foci of tubulin organization, the centers are not connected by microtubules.

The initial appearance of the IMO per se does not result in death. If cells that already contain an IMO are returned to 21°C early in the cell cycle, they remain viable. We propose instead that death occurs when spindle formation is poisoned by the presence of the IMO; that is, microtubules emanating from one of the SPBs aberrantly begin to form a bipolar microtubule array with those from the IMO instead of those from the other SPB. Viability data demonstrate that mispairing during spindle formation occurs in about half the cells, resulting in a broken spindle and death. A further decline in viability that occurs at later stages suggests that even the complete spindles which are formed are defective in some manner that remains to be defined. One potential structural defect in spindles might be that the SPBs lack sufficient bound calmodulin to function properly. Alternatively, formation of the IMO may sequester other SPB components into its own structure, thereby depriving the SPBs of their full complement. We note in this regard that the mutant cells do not enter another cell cycle, and so whatever defect is present appears to be detected by checkpoints for spindle assembly (Hoyt et al., 1991; Li and Murray, 1991).

Why does the IMO appear? One likely scenario is that calmodulin is required to keep the carboxy terminus of Spc110p properly folded for assembly into the SPB. Perhaps the carboxy terminus of the newly synthesized Spc110-220p, which does not bind calmodulin, fails to fold and this leads to aggregation. The amino terminus of Spc110-220p may be unaffected by the folding defect and thus may remain capable of attracting nucleating components, such as the 90-kD component, leading to assembly of the IMO.

Alternatively, delamination of the SPB may nucleate formation of the IMO. That is, calmodulin may be required to anchor Spc110p to the central plaque, thereby mediating the attachment of the inner plaque to the central plaque. The defective binding of calmodulin to Spc110-220p may result in delamination of a portion of the SPB including the mutant Spc110-220p, components of the inner plaque, and nuclear microtubules. This would then act as a seed for growth of the IMO, which is much larger than an inner plaque. If this scenario were true, several arguments indicate that only a small portion of the pole could have delaminated. First, at least some Spc110-220p remains on both poles. At stages following SPB separation, Spc110-220p colocalizes with the 90-kD SPB component even in cells containing two poles and an IMO. Second, both poles often appear by electron microscopy to be normal in the mutant. Finally, although microtubule number is difficult to determine by electron microscopy, both SPBs in the mutant cells generally appear to nucleate the same number of microtubules as wild-type SPBs. It is difficult to imagine that the number of microtubules emanating from each pole would appear similar if a large section of the inner plaque were missing. Unfortunately, the inner plaque of the SPB is not readily detectable by electron microscopy in our preparations, so subtle structural defects might not have been detected.

SPC110 expressed from either a single-copy or a high-copy number plasmid suppresses the temperature sensitiv-

ity of the *spc110-220* homozygous diploid. This complementation of the mutant phenotype is somewhat surprising because the mutant protein on its own is capable of assembling an IMO which disrupts spindle formation. Such behavior might be expected to be dominant, but this is not the case. Although small aberrant structures appear in the nucleus when the heterozygous diploid is shifted to 37°C, they do not nucleate microtubules. One possible explanation for the recessive nature of *spc110-220* is that wild-type Spc110p dimerizes with Spc110-220p to form a functional dimer that can bind calmodulin, permitting normal SPB functions. If the primary defect of Spc110-220p were that it aggregates because the carboxy terminus fails to bind calmodulin, binding to wild-type Spc110p may enhance the solubility of Spc110-220p and thereby prevent its entry into the formation of an IMO.

The temperature-sensitive phenotype of *spc110-220* is similar but not identical to the phenotypes reported for two temperature-sensitive calmodulin mutants, *cmd1-1* (Davis, 1992) and *cmd1-101* (Sun et al., 1992). Neither study employed electron microscopy nor immunofluorescence to investigate the phenotype of the mutant cells at early times after a challenge with the restrictive temperature, so IMOs would not have been detected if they were formed. Recent experiments with a *cmd1-1* homozygous diploid synchronized by elutriation have in fact indicated the presence of IMOs (Sundberg, H.A., L. Goetsch, B. Byers, T.N. Davis, unpublished results). Additionally, although it was previously reported that the spindle in the *cmd1-1* mutant had elongated (Davis, 1992), immunofluorescent staining of the 90-kD SPB component and preliminary electron microscopic analysis now suggests that the spindles actually are broken rather than elongated, just as is seen for the *spc110-220* mutant (Sundberg, H.A., L. Goetsch, B. Byers, T.N. Davis, unpublished results). Analysis of the *cmd1-101* mutant suggested a role for calmodulin in SPB integrity (Sun et al., 1992). Characterization of asynchronous *cmd1-101* cells incubated at the nonpermissive temperature for 4 h revealed that 94% contained only a single SPB and that the majority of those poles were not associated with the nuclear DNA. At 3 h after the shift, however, 15.9% of the cells contained a short spindle, suggesting that SPB duplication had occurred in the *cmd1-101* mutant, but that SPB integrity was defective, thus leading to the loss of one pole (Sun et al., 1992). These reported defects in the calmodulin mutants reflect the inability of Spc110p to assemble appropriately.

Previously in our lab, dominant alleles of *SPC110* were isolated which suppress the temperature-sensitive defects of *cmd1-1*. All dominant suppressors encoded truncations of Spc110p that remove the calmodulin-binding site. The truncated proteins are fully functional in an *spc110Δ* strain. These results suggest that the action of calmodulin during mitosis can be mimicked by truncating Spc110p and removing the calmodulin-binding site (Geiser et al., 1993). Calmodulin is not detected by immunofluorescence at the spindle pole body in strains containing an Spc110p truncation (Davis, T.N., unpublished results), suggesting that calmodulin is not required at the pole for functions unrelated to Spc110p.

The mechanism of suppression by the dominant *SPC110* suppressors is not yet known. However, the fact that re-

moval of the calmodulin-binding site from Spc110p eliminates the need for calmodulin during mitosis is similar to the effects of removing the calmodulin-binding site from several calmodulin-activated enzymes. For example, the calmodulin-activated enzyme myosin light chain kinase (MLCK) contains an active-site inhibitory region that overlaps with the calmodulin-binding site. When calmodulin binds to MLCK, the inhibitory site is removed from the active site and the enzyme is fully functional (Knighton et al., 1992). Furthermore, truncation of MLCK to remove the calmodulin-binding site creates an active, calmodulin-independent enzyme as the inhibitory region overlaps the calmodulin-binding site (Ito et al., 1991). In the same manner, the truncation of Spc110p to remove the calmodulin-binding site may also remove an inhibitory region of Spc110p that blocks the binding of other essential spindle pole components or prevents proper folding of Spc110-220p. In the *spc110-220* mutant, although calmodulin cannot bind to Spc110-220p as in the dominant suppressors, the inhibitory region is still present and thus the requirement for calmodulin binding persists.

In conclusion, we have shown that calmodulin localizes to the central plaque and thus the carboxy terminus of Spc110p is at the central plaque. Characterization of the carboxy-terminal temperature-sensitive allele *spc110-220*, which has a mutation in the calmodulin-binding site, reveals that calmodulin binding to Spc110p is required for the proper assembly of SPB components. At the restrictive temperature, aberrant aggregates of material, which contain the 90- and 110-kD SPB components, form in the nucleoplasm during the time of SPB assembly. These aberrant aggregates, which we have termed intranuclear microtubule organizers or IMOs, are structurally distinct from SPBs, but appear to nucleate microtubules. Spindle formation is poisoned by the presence of the IMO, resulting in loss of cell viability. Future studies characterizing our calmodulin mutants and other Spc110p mutants will be required to define more fully the roles of these proteins in SPB assembly and function.

References

Biggins, S., and M.D. Rose. 1994. Direct interaction between yeast spindle pole body components: Karlp is required for Cdc31p localization to the spindle pole body. *J. Cell Biol.* 125:843–852.

Boeke, J.D., J. Trueheart, G. Natsoulis, and G.R. Fink. 1987. 5-Fluoroorotic acid as a selective agent in yeast molecular genetics. *Methods Enzymol.* 154:164–175.

Brockerhoff, S.E., and T.N. Davis. 1992. Calmodulin concentrates at regions of cell growth in *Saccharomyces cerevisiae*. *J. Cell Biol.* 118:619–629.

Byers, B. 1981. Cytology of the yeast life cycle. *In* The Molecular Biology of the Yeast *Saccharomyces*: Life Cycle and Inheritance. J.N. Strathern, E.W. Jones, and J.R. Broach, editors. Cold Spring Harbor Laboratory Press, Cold Spring Harbor, NY. pp. 59–96.

Byers, B., and L. Goetsch. 1975. Behavior of spindles and spindle plaques in the cell cycle and conjugation of *Saccharomyces cerevisiae*. *J. Bacteriol.* 124:511–523.

Byers, B., and L. Goetsch. 1991. Preparation of yeast cells for thin-section electron microscopy. *Methods Enzymol.* 194:602–608.

Cadwell, R.C., and G.F. Joyce. 1992. Randomization of genes by PCR mutagenesis. *PCR Meth. Appl.* 2:28–33.

Davidow, L.S., L. Goetsch, and B. Byers. 1980. Preferential occurrence of non-sister spores in two-spored asci of *Saccharomyces cerevisiae*: evidence for regulation of spore wall formation by the spindle pole body. *Genetics.* 94: 581–595.

Davis, T. 1990. Genetic analysis of calcium-binding proteins in yeast. *In* Stimulus Response Coupling: The Role of Intracellular Calcium-binding Proteins. V.L. Smith and J.R. Dedman, editors. CRC Press, Boston, MA. pp. 237–249.

Davis, T. 1992. A temperature-sensitive calmodulin mutant loses viability during mitosis. *J. Cell Biol.* 118:607–617.

Davis, T.N., and J. Thorner. 1989. Vertebrate and yeast calmodulin, despite significant sequence divergence, are functionally interchangeable. *Proc. Natl. Acad. Sci. USA.* 86:7909–7913.

Friedman, D.B., H. A. Sundberg, E. Huang, and T.N. Davis. 1996. The 110-kD spindle pole body component of *Saccharomyces cerevisiae* is a phosphoprotein that is modified in a cell cycle–dependent manner. *J. Cell Biol.* In press.

Geiser, J.R., H.A. Sundberg, B.H. Chang, E.G.D. Muller, and T.N. Davis. 1993. The essential mitotic target of calmodulin is the 110-kilodalton component of the spindle pole body in *Saccharomyces cerevisiae. Mol. Cell. Biol.* 13: 7913–7924.

Geiser, J.R., D. van-Tuinen, S.E. Brockerhoff, M.M. Neff, and T.N. Davis. 1991. Can calmodulin function without binding calcium? *Cell.* 65:949–959.

Hoyt, M.A., L. Totis, and B.T. Roberts. 1991. *S. cerevisiae* genes required for cell cycle arrest in response to loss of microtubule function. *Cell.* 66:507–517.

Hoyt, M.A., L. He, K.K. Loo, and W.S. Saunders. 1992. Two *Saccharomyces cerevisiae* kinesin-related gene products required for mitotic spindle assembly. *J. Cell Biol.* 118:109–120.

Ikura, M., G.M. Clore, A.M. Gronenborn, G. Zhu, C.B. Klee, and A. Bax. 1992. Solution structure of a calmodulin-target peptide complex by multidimensional NMR. *Science (Wash. DC).* 256:632–638.

Ito, M., J. Guerriero, V., X. Chen, and D.J. Hartshorne. 1991. Definition of the inhibitory domain of smooth muscle myosin light chain kinase by site-directed mutagenesis. *Biochemistry.* 30:3498–3503.

Kilmartin, J.V., S.L. Dyos, D. Kershaw, and J.T. Finch. 1993. A spacer protein in the *Saccharomyces cerevisiae* spindle pole body whose transcript is cell cycle-regulated. *J. Cell Biol.* 123:1175–1184.

Knighton, D.R., R.B. Pearson, J.M. Sowadski, A.R. Means, L.F. Ten Eyck, S.S. Taylor, and B.E. Kemp. 1992. Structural basis of the intrasteric regulation of myosin light chain kinases. *Science (Wash. DC).* 258:130–135.

Kunkel, T.A., J.D. Roberts, and R.A. Zakour. 1987. Rapid and efficient site-specific mutagenesis without phenotypic selection. *Methods Enzymol.* 154: 367–382.

Lauzé, E., B. Stoelcker, F.C. Luca, E. Weiss, A.R. Schutz, and M. Winey. 1995. Yeast spindle pole body duplication gene *MPS1* encodes an essential dual specificity protein kinase. *EMBO (Eur. Mol. Biol. Organ.) J.* 14:1655–1663.

Li, R., and A.W. Murray. 1991. Feedback control of mitosis in budding yeast. *Cell.* 66:519–531.

Meador, W.E., A.R. Means, and F.A. Quiocho. 1992. Target enzyme recognition by calmodulin: 2.4 Å structure of a calmodulin-peptide complex. *Science (Wash. DC).* 257:1251–1255.

Meador, W.E., A.R. Means, and F.A. Quiocho. 1993. Modulation of calmodulin plasticity in molecular recognition on the basis of x-ray structure. *Science (Wash. DC).* 262:1718–1721.

Mirzayan, C., C.S. Copeland, and M. Snyder. 1992. The *NUF1* gene encodes an essential coiled-coil related protein that is a potential component of the yeast nucleoskeleton. *J. Cell Biol.* 116:1319–1332.

Muhlrad, D., R. Hunter, and R. Parker. 1992. A rapid method for localized mutagenesis of yeast genes. *Yeast.* 8:79–82.

Muller, E.G.D. 1991. Thioredoxin deficiency in yeast prolongs S phase and shortens the G1 interval of the cell cycle. *J. Biol. Chem.* 266:9194–9202.

Pringle, J.R., R.A. Preston, A.E.M. Adams, T. Stearns, D.G. Drubin, B.K. Haarer, and E.W. Jones. 1989. Fluorescence microscopy methods for yeast. *Methods Cell Biol.* 31:357–435.

Roof, D.M., P.B. Meluh, and M.D. Rose. 1992. Kinesin-related proteins required for assembly of the mitotic spindle. *J. Cell Biol.* 118:95–108.

Rose, M.D., and G.R. Fink. 1987. *KAR1*, a gene required for function of both intranuclear and extranuclear microtubules in yeast. *Cell.* 48:1047–1060.

Rout, M.P., and J.V. Kilmartin. 1990. Components of the yeast spindle and spindle pole body. *J. Cell Biol.* 111:1913–1927.

Rout, M.P., and J.V. Kilmartin. 1991. Yeast spindle pole body components. *Cold Spring Harbor Symp. Quant. Biol.* 56:687–691.

Schultz, L.D. 1978. Transcriptional role of yeast deoxyribonucleic acid dependent ribonucleic acid polymerase III. *Biochemistry.* 17:750–758.

Sikorski, R.S., and P. Hieter. 1989. A system of shuttle vectors and yeast host strains designed for efficient manipulation of DNA in *Saccharomyces cerevisiae. Genetics.* 122:19–27.

Spang, A., I. Courtney, U. Fackler, M. Matzner, and E. Schiebel. 1993. The calcium-binding protein cell division cycle 31 of *Saccharomyces cerevisiae* is a component of the half bridge of the spindle pole body. *J. Cell Biol.* 123:405–416.

Spang, A., I. Courtney, K. Grein, M. Matzner, and E. Schiebel. 1995. The Cdc31p-binding protein Karlp is a component of the half bridge of the yeast spindle pole body. *J. Cell Biol.* 128:863–877.

Stirling, D.A., K.A. Welch, and M.J.R. Stark. 1994. Interaction with calmodulin is required for the function of Spc110p, an essential component of the yeast spindle pole body. *EMBO (Eur. Mol. Biol. Organ.) J.* 13:4329–4342.

Sullivan, D.S., and T.C. Huffaker. 1992. Astral microtubules are not required for anaphase B in *Saccharomyces cerevisiae. J. Cell Biol.* 119:379–388.

Sun, G.H., A. Hirata, Y. Ohya, and Y. Anraku. 1992. Mutations in yeast calmodulin cause defects in spindle pole body functions and nuclear integrity. *J. Cell Biol.* 119:1625–1639.

Winey, M., L. Goetsch, P. Baum, and B. Byers. 1991. *MPS1* and *MPS2*: novel yeast genes defining distinct steps of spindle pole body duplication. *J. Cell Biol.* 114:745–754.

Winey, M., M.A. Hoyt, C. Chan, L. Goetsch, D. Botstein, and B. Byers. 1993. *NDC1*: a nuclear periphery component required for yeast spindle pole body duplication. *J. Cell Biol.* 122:743–751.

Wright, A.P.H., M. Bruns, and B.S. Hartley. 1989. Extraction and rapid inactivation of proteins from *Saccharomyces cerevisiae* by trichloroacetic acid precipitation. *Yeast.* 5:51–53.

Wright, R., and J. Rine. 1989. Transmission electron microscopy and immunocytochemical studies of yeast: analysis of HMG-CoA reductase overproduction by electron microscopy. *Methods Cell Biol.* 31:473–512.

Zhu, G., E.G.D. Muller, S.L. Amacher, J.L. Northrop, and T.N. Davis. 1993. A dosage-dependent suppressor of a temperature-sensitive calmodulin mutant encodes a protein related to the *fork head* family of DNA-binding proteins. *Mol. Cell. Biol.* 13:1779–1787.